Margin requirements for first page
Paper size this page A4

122 pt
1.694 in
43 mm

Spatial Position Estimation of Lightweight and Delicate Objects using a Soft haptic Probe

Mohammad Sheikh Sofla, Srikishan Vayakkattil, *Student Member, IEEE*, and Marcello Calisti, *Member, IEEE*

***Abstract*— This paper reports on the use of a soft probe as a haptic exploratory device with Force/Moment (F/M) Readings at its base to determine the position of extremely lightweight and delicate objects. The proposed method uses the mathematical relationships between the deformations of the soft probe and the F/M sensor outputs, to reconstruct the shape of the probe and the position of the touched object. The Cosserat rod theory was utilized in this way under the assumption that only one contact point occurs during the exploration and friction effects are negligible. Soft probes in different sizes were designed and fabricated using a Form3 3D printer and Elastic50A resin, for which the effect of gravity is not negligible. Experimental results verified the performance of the proposed method that achieved a position error between of ~0.7-13*mm*, while different external forces (between 0.01N to 1.5N) were applied along the soft probes to resemble the condition of touching lightweight objects. Eventually, the method is used to estimate position of some points in a delicate card house structure.**

Keywords - Soft probe; Cosserat rod theory; haptic exploration.

54 pt
0.75 in
19.1 mm

I. Introduction

In the last decade, robots moved from highly controlled environments such as assembly lines to unstructured and natural environments [1]-[3]. In this way, robots need to sense their surroundings and be able to plan specific actions such as accurate manipulation and effective locomotion. Cameras and range sensors are the common tools employed to explore the environment, but their effectiveness can be limited in the presence of occlusions (e.g. vegetation), in foggy environments, underwater or when the working lighting conditions are different from the testing lighting conditions [4], [5]. In this regard haptic exploration, i.e. the employment of physical contact to understand a scene, provides a good alternative and it can also enable the robot to retrieve specific information such as mass and stiffness from the object [6], [7]. However, very delicate or lightweight objects can be easily damaged by physical contact. So appropriate control algorithms, extremely sensitive sensors, slow movements, and high computational resources are required. Even by the delicate contacts of the state of the art tactile sensors, high-value and delicate objects can be easily damaged, especially in conditions where the robot cannot explicitly infer the object position [8], and this is proved challenging with traditional haptic robotic approaches.

Over the past decade, researchers have investigated the employment of soft and elastic materials (e.g. rubbers, silicones or hydrogels) to build robots [9]-[11]. This has evolved into a novel branch of robotics called soft robotics that exploits the deformability of soft bodies to gently interact with the environment. In such a way, safe interaction is guaranteed by the mechanical deformations of the body of the robot, rather than relying on expensive sensors and accurate control algorithms [12]. Soft robotic structures deform significantly when subject to external forces, and are considered inherently safe when interacting with fragile objects.

The approach followed in this paper is to combine haptic and soft robotics to enable a robotic system to understand the environment, specifically in context where range sensors are ineffective and rigid haptic systems might damage delicate objects (e.g. soft fruits harvesting, biological specimens collection, medical examinations, etc.). The idea is to use a soft flexible rod, called here Soft Probe, to sense the environment and provide position feedback. However, the high degree of deformation of soft structures impairs traditional sensing methodologies, and several research efforts are ongoing to fill this gap [13]-[14].

37 pt
0.514 in
13.1 mm

In general, to retrieve objects position from contacts the shape of the probe and the position along the probe where the contact happened are needed. Shape reconstruction is performed by embedding sensors capable of retrieving certain properties of the probe, for example curvature, twist, elongation or strain [14]. When global properties are retrieved for the whole probe, approximating assumptions are used, such as constant curvature/twist or no-shear. But such assumptions hold only on a specific subset of probes. When properties are retrieved locally, model-based or model-free reconstructions are needed, the accuracy of which increases as the number of sensors increases [15]. In such cases, the network of embedded sensors influences the Young module, and it carries challenges such as modelling the heterogeneous system, identifying the best positions of the sensors, wiring them, and integrating the data.

Contact sensors for soft robots are often borrowed from wearable devices and electronic skins [13]. Recently, continuous approaches like Fiber Bragg Grating sensors enables retrieval of contacts on large surfaces with a reduced number of transducers [16], but the need of an external interrogator and the non-stretchability of such systems limits the field of application. Moreover, the highest touch sensitivity ($\sim 10^{-2}$N) still requires an array of sensors [17], which have the aforementioned limitations. Therefore, integration of both shape reconstruction and contact sensors reduces the capability of soft probes to detect extremely lightweight and delicate objects (e.g. berries, soft corals, etc.). Without advances in sensing technologies, soft probes for haptic exploration (i.e.

Mohammad Sheikh Sofla (msofla@lincoln.ac.uk), Srikishan Vayakkattil (25653308@students.lincoln.ac.uk) and Marcello Calisti (corresponding author, mcalisti@lincoln.ac.uk), are with the Lincoln Institute for Agri-Food Technology, College of Science, University of Lincoln, Lincoln LN2 2LG, U.K. This work was supported by Research England (Lincoln Agri-Robotics) as part of the Expanding Excellence in England (E3) Program.

54 pt
0.75 in
19.1 mm

the retrieval of the position or properties of an object by using haptic information alone) have limited applications.

The method proposed in this study uses a small six-axis Force/Moment (F/M) sensor (at the base of the soft probe for reconstruction of its shape and identification of the position of the touched object as well. This strategy will not embed components into the soft probe, so that the compliance can be maximized. The concept of using base sensors to retrieve contact and shape information is already known in robotics. Seminal research has shown that contact position along thin rods can be identified with force/torque information at the base [18]. This result boosted the use of antennae or whisker-inspired sensors [19]. For example, Nitinol ($E \approx 80$ GPa) wire is used to determine shape of rigid objects with base readings [20], [21]. Although object detection mediated by touch has been demonstrated in whisker-inspired sensors (made of thin plastic or steel rods) [22], studies to date employ small deflection approaches and ignore gravity. These assumptions are unsuitable for the significant deformations that soft robots are characterized by, preventing the extension of previous findings to soft probes. Precisely obtaining the contact position and shape when the probe is made of soft materials, e.g. for soft robots and grippers, is challenging. Two recent studies address more significant deformations [23], [24], but also in these cases, tip load (e.g. clamped end) and no gravity assumptions limit their applicability.

In the present study, the gravity effects are considered and the applied external force from the touched object could be in any position along the soft probe (not just the tip). However, it is assumed that the contact happens at only one position, while the friction effects are negligible. The proposed method could provide new exploration capabilities for soft grippers, applicable to several natural settings (e.g. agricultural fields, forests, coral barriers) and greatly improving performance of different tasks (e.g. manipulation, object recognition, properties inference). Experimental studies verify the performance of this method to predict the shape of the soft probes in no load and different loading conditions, as well as the position of the applied contact force. To the author knowledge, this is the first time an F/M base sensor alone is used to identify contact positions along a soft probe (E <3 MPa) considering the gravity effects.

II. Proposed Method

When a probe touches an object, it is possible to determine the position of the latter with respect to the base of the former by means of the contact position and the shape of probe. So, the proposed method tries to estimate the shape of probe and also the contact point of the applied external force along the probe, by using F/T readings at the base, under the assumptions that only one frictionless contact occurs.

As a result of these assumptions, only one external force may be applied along the probe, and we assume no external moments. The shape of probe can be described as its centerline curve Cartesian position in space ($\boldsymbol{P}$), and the rotation matrix of its orientation ($\boldsymbol{R}$), as functions of a reference parameter (s), which is the arclength of the probe. The shape is measured in a frame attached to the base of the probe. An accurate model is needed to calculate the shape and Cosserat rod theory is a proper choice for this purpose [24]. The static model of the elastic probe (straight when there is no external and

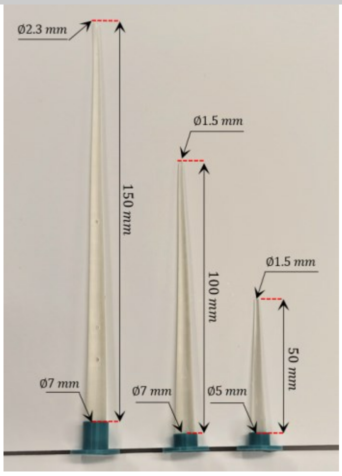

Figure 1. Sizes of the fabricated large, medium and small probes.

gravitational forces), based on the Cosserat rod theory is described by the following ODEs:

$$\begin{gathered} \boldsymbol{v} = {\boldsymbol{K}_{se}}^{-1}\boldsymbol{R}^{\mathrm{T}}\boldsymbol{n} + [0 \quad 0 \quad 1]^{\mathrm{T}} \\ \boldsymbol{u} = {\boldsymbol{K}_{bt}}^{-1}\boldsymbol{R}^{\mathrm{T}}\boldsymbol{n} \\ \boldsymbol{P}_s = \boldsymbol{R}\boldsymbol{v} \\ \boldsymbol{R}_s = \boldsymbol{R}\hat{\boldsymbol{u}} \\ \boldsymbol{n}_s = \rho A[\mathrm{g} \quad 0 \quad 0]^{\mathrm{T}} + \boldsymbol{F}_e\delta(s - s_e) \\ \boldsymbol{m}_s = \boldsymbol{P}_s \times \boldsymbol{n} \end{gathered} \tag{1}$$

where $\boldsymbol{v}$ is the rate of change of position with respect to arclength and $\boldsymbol{u}$ is the curvature vector, both defined in the local frame, and $\boldsymbol{n}$ and $\boldsymbol{m}$ are the internal force and moment in the global frame, respectively. $\boldsymbol{F}_e$ is the applied external force, and $\delta(.)$ is the Dirac delta function. $\boldsymbol{K}_{se}$ is the stiffness matrix for shear and extension, and $\boldsymbol{K}_{bt}$ represent the stiffness matrix for bending and twisting, defined as follow

$$\boldsymbol{K}_{se} = \begin{bmatrix} GA & 0 & 0 \\ 0 & GA & 0 \\ 0 & 0 & EA \end{bmatrix}, \boldsymbol{K}_{bt} = \begin{bmatrix} EI_{xx} & 0 & 0 \\ 0 & EI_{xx} & 0 \\ 0 & 0 & GI_{zz} \end{bmatrix}. \tag{2}$$

where A is the cross-sectional area of the probe, and E and G are the Young's modulus and the Shear modulus, respectively. To solve these ODEs and determine the shape of probe, the amounts of force and moment at the origin ($\boldsymbol{n}(0)$ and $\boldsymbol{m}(0)$) are needed and could be measured via the available 6 axis F/M sensor at the base. However, also the amount of the applied external force ($\boldsymbol{F}_e$) and contact point of the force along the probe arclength (s_e) must be determined. The relationship between the F/M sensor readings at the base ($\boldsymbol{F}_b$ and $\boldsymbol{M}_b$), and the applied forces (gravitational force and the applied external force) along the probe can be described by

$$\begin{gathered} \boldsymbol{F}_b = \boldsymbol{R}^{\mathrm{T}}(\boldsymbol{F}_e + m[\mathrm{g} \quad 0 \quad 0]^{\mathrm{T}}), \\ \boldsymbol{M}_b = \boldsymbol{R}^{\mathrm{T}}(\boldsymbol{P}_e \times \boldsymbol{F}_e + \boldsymbol{P}_c \times m[\mathrm{g} \quad 0 \quad 0]^{\mathrm{T}}), \end{gathered} \tag{3}$$

where $\boldsymbol{P}_e$ and $\boldsymbol{P}_c$ are the positions of the applied external force and the probe center of mass, respectively. The variable m is the total mass of the probe and g stands for the gravitational acceleration. If the force sensor reading was in the determined range for gravity effect as

$$\boldsymbol{F}_b = m\boldsymbol{R}^{\mathrm{T}}[\mathrm{g} \quad 0 \quad 0]^{\mathrm{T}}, \tag{4}$$

then, it means there is not an external force or the applied external force is negligible. But, if the force sensor readings exceeded the gravity effect, so the presence of an external force is detected and then the amount and the contact point of the force should be determined. The amount of the external force could be determined by subtracting the gravity effect from force sensor output as follow

$$\boldsymbol{F}_e = \boldsymbol{R}\boldsymbol{F}_b - m[\mathrm{g} \quad 0 \quad 0]^{\mathrm{T}}. \tag{5}$$

Now, the contact point along the probe (s_e) must be determined using the outputs of the moment sensor. But, the moments at the base are also dependent on the probe shape and the exact shape of the probe is still unknown.

However, under the assumption of no external moments, the moment at the tip of the probe is expected to be zero. So, we have a boundary value problem and the shooting method could be utilized to change the problem into an initial value problem. By using the shooting method technique, the actual shape of probe that satisfies the zero-moment condition at the tip will be determined, as well as the contact point of the applied force (and therefore the approximate position of the touched object). The performance of the proposed method is investigated in the next section.

III. Experimental Procedure

Three soft conic probes of different sizes were used as soft haptic probes in these experiments. The probes are made of Elastic 50A and printed using Form 3, washed for 20 minutes and post-cured with Form Cure at 60 ˚C for 20 minutes. The sizes of the printed probes are given in Figure 1. An ATI Nano17 F/M sensor is used as sensor for the shape and position estimation. The sensor is mounted at the base of probes and 3D printed elements connect each probe to the sensor. A metal blade is used to apply the external forces along the probes in the experiments. The experimental setup is shown in Figure 2. The proposed estimation algorithm is implemented in Matlab. In order to validate the proposed method, the estimated shape of the probes and the estimated positions of the applied contact forces are compared with the reconstructed ones using two cameras (DSC-RX100M4, Sony) in stereo configuration and using a Direct Linear Transformation (DLT) approach [23]. As reconstruction setup for the DLT, we used a calibration box with 20 calibration points, while markers were placed equidistantly (~1cm) on the Soft Probe.

The tests done in this research were divided in different main categories. For the first category, we did some tests in the absence and presence of different external loads to identify the properties of the probe's material (E and G), using the least squares parameter estimation [24]. The other mechanical properties (dimensions and density), are measured with physical investigations. Then we did preliminary tests to evaluate the feasibility of the approach. In the second category, we ran an experimental campaign in which we touched the three probes in horizontal position, from x, y and z directions as highlighted in Figure 2, and with different force intensities from 0.005N to 1.5N. A total of 25 experiments were performed, for which we used the methods mentioned before to establish shape reconstruction and contact position errors. In the experiments, the Root Mean Square (RMS) error for the shape estimation is obtained with the following equation

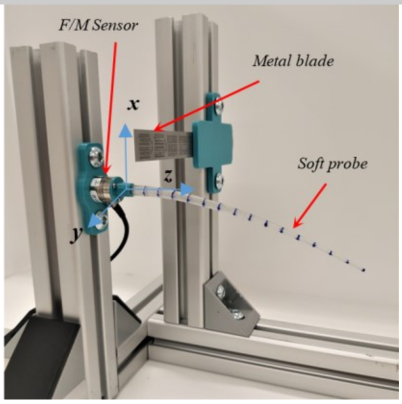

Figure 2. The experimental setup with the reference frame used.

$$e_{rms} = \sqrt{\frac{1}{N}\sum_1^N (\boldsymbol{P}-\bar{\boldsymbol{P}})^{\mathrm{T}}(\boldsymbol{P}-\bar{\boldsymbol{P}})}. \tag{6}$$

where N is the number of the measured points and $\bar{\boldsymbol{P}}$ is the reconstructed marker position. The position error of the contact point is evaluated as the Euclidean distance between the estimated contact point, and the reconstructed one with the DLT method. For the last category, we use the proposed method to identify the position of a house of cards based on the estimated contact position explained above. Here, instead of keeping fixed the position of the base of the probe, we moved it until we touched the object, and then we reconstructed the relative position of the touched object with respect to the base of the probe.

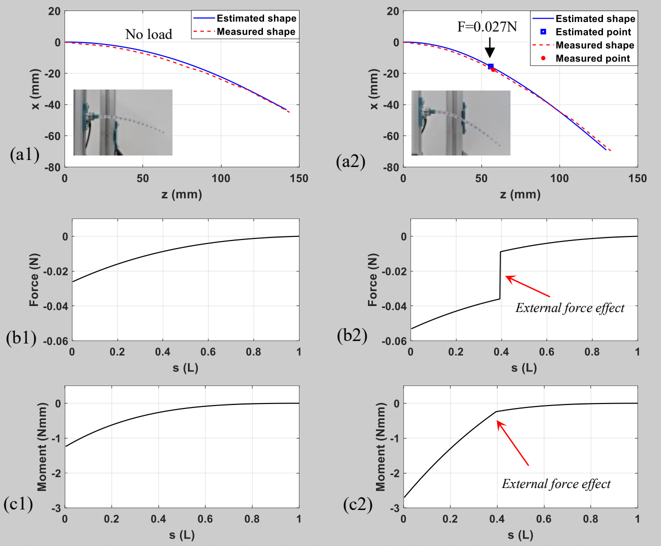

Figure 3. The measured and estimation results for the large probe in (a1) no-load condition and (a2) when a downward load is applied to the probe, with the estimated (b1 and b2) forces and (c1 and c2) moments along the probe.

IV. Experimental Results

The identification of the Young's modulus ($E = 2.32 \times 10^6$ Pa) and the Shear modulus ($G = 7.61 \times 10^5$ Pa), allowed us to find the stiffness matrixes ($\boldsymbol{K}_{se}$ and $\boldsymbol{K}_{bt}$), as per Eq. 2. Then, the large probe shape is estimated with the Cosserat rod model, under the gravitational force and in no external load condition, and it is compared with the measured results using reconstructed markers position, as per in Figure3(a1). The RMS error for the shape estimation has been of 3.62mm. A similar figure, (RMS=3.84mm) has been obtained when a downward force of 0.014N is applied to the probe at 60mm arc-length distance from its base (0.4 L), as shown in Figure 3(a2). The estimated point of the external force is also shown in Figure 3(a2), and is compared with the measured one. An error of 2.6mm has been obtained. The estimated internal forces and moments for the both tests are also given in Figures 3(b) and 3(c). The force variations for the no external load condition (see Figure 3(b1)) comes from the variation of gravitational forces along the conic probe, while the applied external load can cause a sudden variation in the estimated force at the position that the force is applied (see Figure 3(b2)). The applied external force caused a jump in the moment curve, as shown in Figure 3(c2). These preliminary tests showed that the proposed method can estimate the shape of the probe under the gravitational force, as well as the contact position of the applied external force.

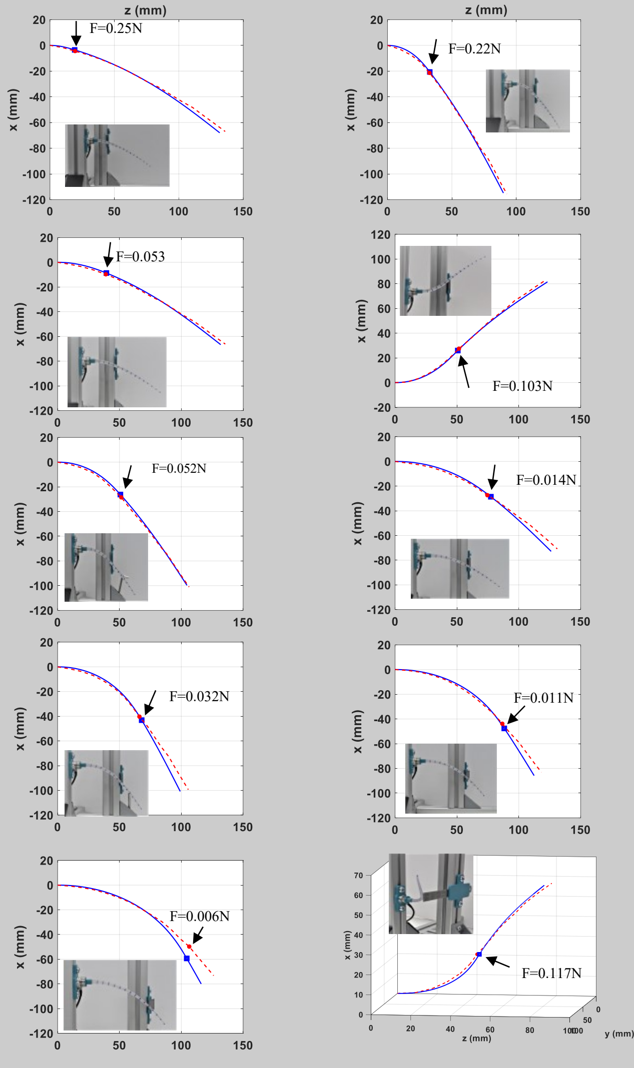

Figure 4. The experimental results for applying different forces on the large probe. The reconstructed shape of the probe (----) and position of the external force (●), with the estimated shape (——) and the position of external force (■) using the proposed method.

In the next experiments, the metal blade is mounted in different positions with respect to the fabricated probes and external forces are applied at different points and in different directions, as described in the Experimental Procedure section. The graphs in Figure 4 show the results for the large probe. As it appear from visual inspection of the estimated vs reconstructed shapes, the amount of error increases as the applied external force approaches the end of the probe. Near the tip, very low forces are needed to change the shape of the probe and so the probe will apply negligible forces to the environment. However, since the measured forces decreased below 0.01N, the effect of sensor errors in the estimation process increased drastically. Figures 5 and 6, show the test results for the medium and small probes, respectively.

We identified two main causes for the error in the contact point: the first one is related to a miss-reconstruction of the probes. When the error in shapes is close to the contact point, it can be appreciated via visual inspection (for example from Figure 4, bottom row) that the error is intrinsic of the shape reconstruction. A second source of error is related to the shooting method, which found the contact point in another position of the arc length of the probe. This can be identified from the visual inspection of bottom rows of Figure 5 and Figure 6.

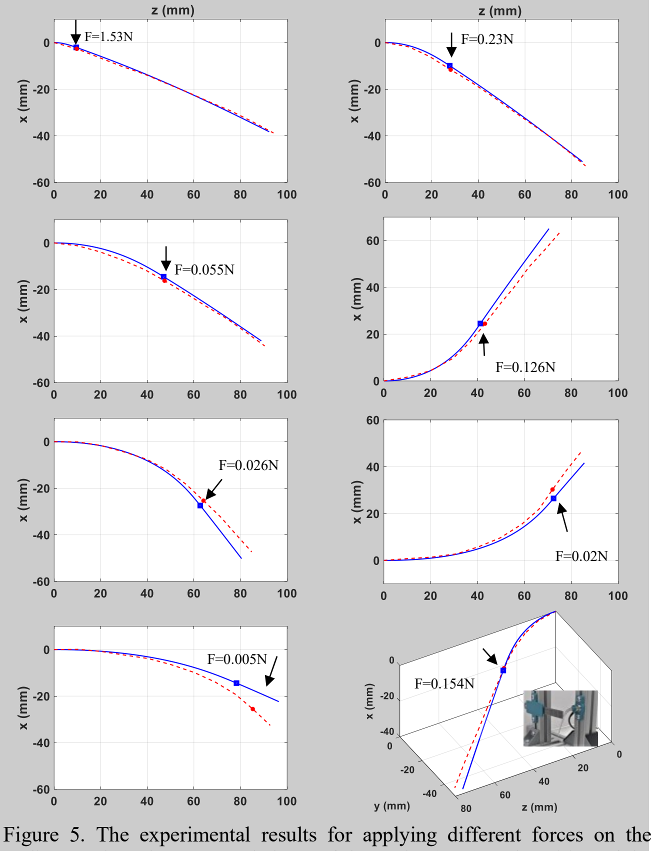

Figure 5. The experimental results for applying different forces on the medium probe. The measured shape of the probe (----) and position of the external force (●), with the estimated shape (——) and the position of external force (■) using the proposed method.

Table 1 summarizes the RMS values of the shape estimation error in both millimeters and as a percent of the probe's length, as well as the absolute error in contact point estimation of the applied external forces. From the results, it can be concluded that when the applied force from the touched object is more than 0.01N, the position estimation error of the proposed method is confined within 5mm. From Table 1, it is also clear that the error in estimation of the contact point increases as the tip of the probes is used to touch the object. This was reasonably expected since both the shape and arc length errors will increase, resulting in an overall greater error. However, in the large probe, the shape estimation error as a percent of the probe length was less than the others. This is since the RMS is similar in absolute value for the different probes, but then the length will influence the RMS%. It is still not clear if the similar RMS is obtained as a limitation of the reconstruction algorithm or if other reasons have to be investigated. However, from our experiments it seems that the long probe is the most suitable geometry, which combines similar error in contact position with the smaller probes, with lower forces needed for deforming it. This implies that we should focus, in the next steps of this research, on the employment of torque readings only if we want to minimize the force exerted to the object.

TABLE I

ESTIMATION ERROR RESULTS

	Applied force		Estimation results		
	Amount (N)	Contact point (L)	Shape RMS error* (*mm*)	Shape RMS error* %	Contact point error (*mm*)
Large probe	0.25	0.133	3.64	2.42	1.14
	0.22	0.266	3.68	2.45	1.43
	0.053	0.266	3.81	2.54	1.25
	0.103	0.4	3.74	2.49	1.88
	0.052	0.4	3.84	2.56	2.41
	0.014	0.533	4.17	2.78	3.06
	0.032	0.533	4.51	3.00	3.35
	0.011	0.666	4.06	2.70	4.08
	0.006	0.8	5.67	3.78	9.78
Medium probe	1.5	0.1	3.78	3.78	0.68
	0.23	0.3	4.15	4.15	1.76
	0.126	0.5	4.78	4.78	1.96
	0.055	0.5	4.39	4.39	1.77
	0.26	0.7	4.25	4.25	2.51
	0.02	0.8	4.78	4.78	3.84
	0.005	0.9	5.83	5.83	13.14
Small probe	0.4	0.2	4.51	9.02	0.67
	0.11	0.4	4.21	8.42	0.88
	0.2	0.4	4.33	8.66	1.18
	0.07	0.6	4.67	9.34	1.42
	0.047	0.6	4.43	8.86	1.28
	0.083	0.6	4.26	8.52	2.52
	0.032	0.8	4.14	8.28	4.17

* The error is presented in *mm* and in % with respect to the length of the probe

Eventually, in the last test, the large probe is used to touch a delicate card house and measure some points in the structure as shown in Figure 7(a). Very low forces should be applied to touch such delicate structure without collapse (see also the video in the supplementary material). Figure 7 (b) compares the estimation results of the proposed method with the video measurements. In these tests, the applied forces were below 0.01N, and moments were up to 1Nmm. The point estimation errors in the card house test were confined within 12mm: even if the value is significant, it is within a suitable value to use a soft gripper. Precise positions are not required for performing delicate grasping with most of soft grippers, and we believe that an error of about 1cm can be a good estimated to perform a grasp without the need of additional position information.

Moreover, Figure 8 shows the variation of the forces and moments during the first touch of the card house structure (the filtered output of the F/M sensor). In the first part of the plots, moving the probe to reach the desired point cause infinitesimal variations in the force reading. In the touching phase, the force and moment outputs start to change, and then in the static condition the probe is not moving to collect data for the estimation process. The measured forces in Figure 8 are very low, but the amount of the measured moments are considerable. The estimation error of the proposed method increases when the probe touches the objects near the tip with trivial forces, due to the inability of the employed sensor to accurately measure the forces less than 0.01N.

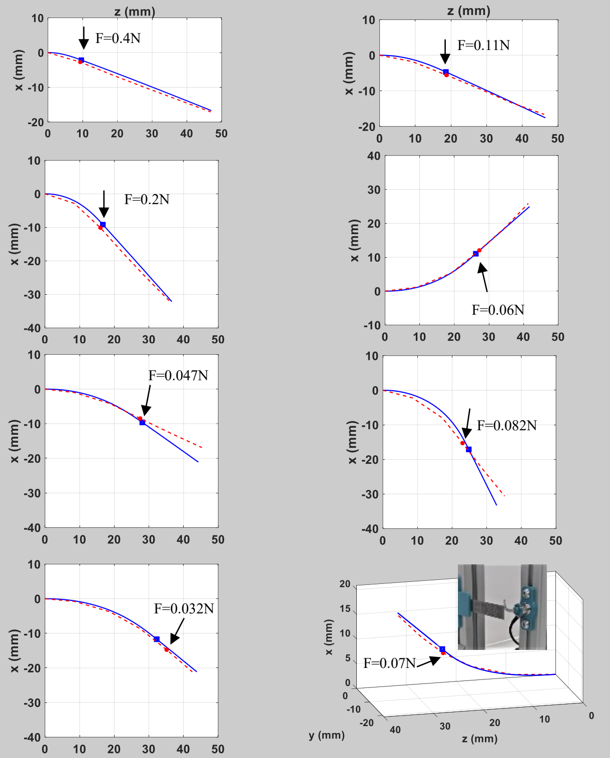

Figure 6. The experimental results for applying different forces on the small probe. The measured shape of the probe (----) and position of the external force (●), with the estimated shape (——) and the position of external force (■) using the proposed method.

However, with touching near the tip, the moments in base are significant and the F/M sensor can read them with proper accuracy. In the future work, our team will focus on soft probe position estimation with just moment reading at the base and touching one point several times with moving the probe, in the hope of reducing even further the amount of force that can be applied to the environment, and in the meantime to increase the estimation of the contact point position. Moreover, we plan to use the proposed technology in a soft gripper to have an exploratory hand [28], to perform sensing and grasping.

V. CONCLUSION

A novel method is developed here to identify and interact safely with complex surroundings, going beyond the previous attempt with steel or plastic whiskers, which usually neglect gravity or use as assumption a tip contact. The proposed estimation method could calculate the shape of the probe as well as position of the external force, even in presence of gravity. Experimental investigations verified that the proposed method can predict the position of external objects by applying very small forces and with reasonable errors. The method applied here for a soft flexible probe can be extended to other shapes and devices, and it is not linked specifically to the Cosserat model, but to any approach which can retrieve the shape of the robot/finger and can estimate the internal force and moments. The proof that base readings are enough for this task, will pave the way to new investigations on how soft robots can maximize their compliance, without any additional rigid element, and at the same time obtain accurate awareness of the surrounding environment.

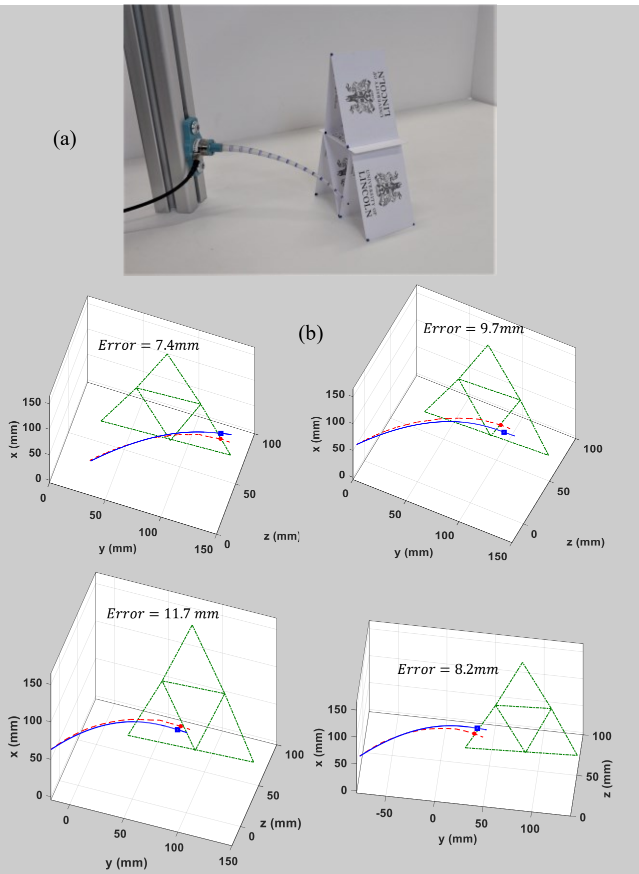

Figure 7. (a) Touching a card house with the large probe; (b) The measured shape of the probe (----) and the measured position of the touched point (●), with the estimated shape (——) and the estimated position of touched point (■) using the proposed method.

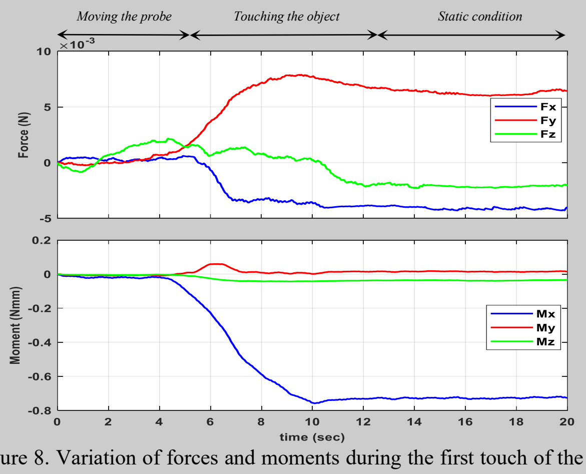

Figure 8. Variation of forces and moments during the first touch of the card house structure.

REFERENCES

[1] G. Z. Yang *et al.*, 'The grand challenges of science robotics,' *Science robotics*, vol. 3, no. 14, eaar7650, 2018.

[2] J. Liu, S. Iacoponi, C. Laschi, L. Wen and M. Calisti, 'Underwater mobile manipulation:A soft arm on a benthic legged robot,' *IEEE Robotics Automation Magazine*, vol. 27, no. 4, pp. 12–26, 2020.

[3] M. S. A. Mahmud, M. S. Z. Abidin, A. A. Emmanuel and H. S. Hasan, 'Robotics and automation in agriculture: Present and future applications,' *Applications of Modelling and Simulation*, vol. 4, pp. 130–140, 2020.

[4] K. Kapach, E. Barnea, R. Mairon, Y. Edan and O. Ben-Shahar, 'Computer vision for fruit harvesting robots–state of the art and challenges ahead,' *International Journal of Computational Vision and Robotics*, vol. 3, no. 1-2, pp. 4–34, 2012.

[5] L. Bruzzone and G. Quaglia, 'Review article: Locomotion systems for ground mobile robots in unstructured environments,' *Mechanical Sciences*, vol. 3, no. 2, pp. 49–62, 2012. doi: 10.5194/ms-3-49-2012.

[6] M.M. Sreekanth and R. Kannan Megalingam, 'Haptic solutions for agriculture,' in *2018 International Conference on Computing, Power and Communication Technologies (GUCON)*, 2018, pp. 416–420.

[7] S. A. Stansfield, 'Haptic perception with an articulated, sensate robot hand,'*Robotica*, vol. 10, no. 6, pp. 497–508, 1992.

[8] M. H. Lee, 'Tactile sensing: New directions, new challenges,' *The International journal of robotics research*, vol. 19, no. 7, pp. 636–643, 2000.

[9] N. Sinatra, C. Teeple, D. Vogt, K. Parker, D. Gruber and R. Wood, "Ultragentle manipulation of delicate structures using a soft robotic gripper", Science Robotics, vol. 4, n. 33, 2019.

[10] M. S. Sofla, M. J. Sadigh, M. Zareinejad, "Design and dynamic modeling of a continuum and compliant manipulator with large workspace", Mechanism and Machine Theory, Vol. 164, 104413, 2021.

[11] M. S. Sofla, M. J. Sadigh, M. Zareinejad, "Shape estimation of a large workspace continuum manipulator with fusion of inertial sensors," Mechatronics, Vol. 80, 102684, 2021.

[12] M. Calisti, M. Giorelli, G. Levy, B. Mazzolai, B. Hochner, C. Laschi, P. Dario "An octopus-bioinspired solution to movement and manipulation for soft robots," Bioinspiration & biomimetics, 2011.

[13] B. Shih, D. Shah, J. Li, T. Thuruthel, Y. Park, F. Iida, Z. Bao, R. Kramer-Bottiglio e M. Tolley, 'Electronic skins and machine learning for intelligent soft robots,' Science Robotics, vol. 5, n. 41, 2020.

[14] H. Wang, M. Totaro e L. Beccai, 'Toward perceptive soft robots: Progress and challenges,' Advanced Science, vol. 5, n. 9, 2018.

[15] K. Chin, T. Hellebrekers e C. Majidi, 'Machine learning for soft robotic sensing and control,' Advanced Intelligent Systems, vol. 2, no. 6, p. 190071, 2020.

[16] L. Massari, E. Schena, C. Massaroni, P. Saccomandi, A. Menciassi, E. Sinibaldie C. Oddo, 'A machine-learning-based approach to solve both contact location and force in soft material tactile sensors,' Soft Robotics, vol. 7, n. 4, pp. 409-420, 2020.

[17] Y. Tenzer, L. Jentoft e R. Howe, 'The feel of MEMS barometers: Inexpensive and easily customized tactile array sensors.' IEEE Robotics & Automation Magazine, vol. 21, n. 3, pp. 89-95, 2014.

[18] T. Tsujimura e T. Yabuta, «Object detection by tactile sensing method employing force/torque information,» IEEE Transactions on robotics and Automation, vol. 5, n. 4, pp. 444-450, 1986.

[19] M. Kaneko, N. Kanayama e T. Tsuji, «Active antenna for contact sensing,» IEEE Transactions on robotics and automation, vol. 14, n. 2, pp. 278-291, 1998.

[20] J. H Solomon and M. Hartmann. "Extracting object contours with the sweep of a robotic whisker using torque information". The International Journal of Robotics Research, 2010, 1233-1245.

[21] M. A. Lin, E. Reyes, J. Bohg and M. R. Cutkosky, "Whisker-Inspired Tactile Sensing for Contact Localization on Robot Manipulators," *International Conference on Intelligent Robots and Systems*, Kyoto, Japan, pp. 7817-7824, 2022.

[22] D. Kim e R. Möller, «Biomimetic whiskers for shape recognition,» Robotics and Autonomous Systems, vol. 55, n. 3, pp. 229-243, 2007.

[23] R. Takano, H. Mochiyama e N. Takesue, «Real-time shape estimation of Kirchhoff elastic rod based on force/torque sensor,» ICRA, 2017.

[24] S. Sadati, A. Shiva, N. Herzig, C. Rucker, H. Hauser, I. Walker, C. Bergeles, «Stiffness imaging with a continuum appendage: real-time shape and tip force estimation from base load readings,» IEEE Robotics and Automation Letters, vol. 5, n. 2, pp. 2824-2831, 2020.

[25] J. Till, V. Aloi, and C. Rucker, "Real-time dynamics of soft and continuum robots based on Cosserat rod models," Int. J. Rob. Res., vol. 38, no. 6, pp. 723–746, 2019.

[26] T. L. Hedrick, "Software techniques for two- and three-dimensional kinematic measurements of biological and biomimetic systems". *Bioinspiration & Biomimetics,* 2008*,* 3, 034001.

[27] K. J. Astrom and B. Wittenmark, "Adaptive Control". Addision-Wesley Publishing Company, 1934.

[28] M. A. Lin, R. Thomasson, G. Uribe, H. Choi and M. R. Cutkosky, "Exploratory Hand: Leveraging Safe Contact to Facilitate Manipulation in Cluttered Spaces," in *IEEE Robotics and Automation Letters*, vol. 6, no. 3, pp. 5159-5166, 2021.